AgNPs functionalized with dithizone for the detection of Hg2+ based on surface–enhanced Raman scattering spectroscopy

Na Guo
Liaoning University
Guangda Xu
Liaoning University
Qijia Zhang
Liaoning University
peng song (songpeng@lnu.edu.cn)
Liaoning University https://orcid.org/0000-0003-3093-0068
Lixin Xia
Liaoning University

Research Article

Keywords: Hg2+, SERS, dithizone, sensor, water analysis

Posted Date: January 12th, 2022

DOI: https://doi.org/10.21203/rs.3.rs-1224290/v1

Abstract

Mercuric ion (Hg^{2+}), a poisonous metal ion that remained in water ecosystems, can severely damage the human central and peripheral nervous system and kidneys. Consequently, rapid and highly sensitive methods to determine trace Hg^{2+} are meaningful to discuss. We have proposed a novel approach of surface-enhanced Raman scattering (SERS) for the quantitative analysis of Hg^{2+} in water samples using dithizone (DTZ) as a Raman reporter. DTZ-modified silver nanoparticles (AgNPs) produced a strong SERS signal. In the presence of Hg^{2+}, the DTZ can capture Hg^{2+} composing a stable structure, resulting in DTZ leaving the surface of the AgNPs, with an accompanying decrease in the signal. The proposed SERS assay showed a linear range of 10^{-4}–10^{-8} M, with a limit of detection of 9.83×10^{-9} M. The sensor has low detection cost, rapid detection speed, and uncomplicated sample pretreatment. Furthermore, this method can be successfully utilized to detect Hg^{2+}rapidly in water samples, which sheds new light on the detection of Hg^{2+} in the environment.

1. Introduction

Heavy metals have a considerable impact on soil, plants, aquatic animals and humans [1, 2]. Hg^{2+} is one of the heavy metal ions, which is highly toxic in organisms and ecosystems even at a low concentration of 5 μg/L [3]. Mining activities, municipal waste, oil and coal combustion, cement production, consumer product emissions, waste–water emissions and so on are the major sources of mercury ion emissions into the environment, which has caused pollution due to improper treatment methods [4, 5]. Hg^{2+} poisoning can cause neurological, renal, immune, cardiac, sports, reproductive and genetic diseases in humans [6–8]. Therefore, it is of great significance to study the widespread distribution of Hg^{2+} in the aquatic environment and bioaccumulation in the food chain [9–11].

At present, many analysis techniques have been utilized in the detection of Hg^{2+} such as atomic absorption spectrometry, inductively coupled plasma-mass spectrometry (ICP–MS), high-performance liquid chromatography, electrochemistry, colorimetry and fluorescence spectroscopy [12–19]. However, these methods have limitations [20, 21], such as complex sample preparation, expensive equipment and time-consuming procedures. Therefore, a simple, highly selective and sensitive method for measuring Hg^{2+} must be developed to overcome these shortcomings. A nondestructive optical inspection is an attractive option, it can respond quickly in natural environments and organisms.

Surface–enhanced Raman scattering (SERS) is a non-destructive and rapid analysis technique that has a wide range of applications [21–24], especially the analysis of trace poisonous substances, such as heavy metal ions, dyes and pesticides [25–28]. In recent years, using SERS to detect Hg^{2+} has received widespread attention. Various methods have been proposed by sveral groups for detecting Hg^{2+}, based on different SERS probes. Qi et al. studied a T–Hg^{2+}–T mismatch base pair pattern for Hg^{2+} detection [29]. Hao et al. reported that acridine yellow was used to detect Hg^{2+} quantitatively because of the interaction between acridine yellow and silver nanoparticles (AgNPs) [4]. Luo et al. introduced safranine T

as a SERS probe, allowing trace analysis of Hg^{2+} with high selectivity [17]. Although these methods achieve the advantages of rapid and sensitive detection of Hg^{2+}, they are susceptible to biological and environmental influences.

Herein, we employed a SERS assay for the rapid, selective, and sensitive analysis of Hg^{2+} in water samples. In this work, indirect SERS detection of Hg^{2+} is carried out based on dithizone (DTZ) as a Raman probe. The quantitative decrease of the SERS signal of the probe molecule of DTZ was observed when DTZ–functionalized AgNPs were mixed with a certain amount of Hg^{2+}, which suggests that the phenomenon of decreased SERS signal intensity should be mainly attributed to the interaction between Hg^{2+} and DTZ [30, 31]. This quantitative detection strategy of the proposed method is shown in Figure 1.

2. Materials And Methods

2.1 Chemicals and reagents

All reagents and solvents were of analytical grade, and no further purification is required when used. DTZ, absolute ethanol, sodium citrate, $AgNO_3$, $HgCl_2$, KNO_3, $Al(NO_3)_3$, $Fe(NO_3)_3$, $Bi(NO_3)_3$, $Cu(NO_3)_2$, $NaNO_2$, $Ni(NO_3)_2$ and $Pb(NO_3)_2$ were all purchased from China Energy Chemical Co., Ltd. The solutions used in this experiment were prepared using deionized water.

2.2 Instrumentation

A JEM–2100 ultra–high–resolution transmission electron microscope (JEOL, Japan) was used to characterize AgNPs, and to determine the geometry and size of the AgNPs. A PerkinElmer Lambda 35 spectrophotometer (326 nm; Norwalk, CT, USA) was used to record the ultraviolet–visible (UV–vis) absorption spectra. The SERS measurements was performed using a Renishaw InVia Reflex confocal microscope (Renishaw, UK). All measurements were performed using a He–Ne laser (532 nm, exposure time of 10 s). The laser spot diameter was 1 μm, and the laser power was 50 mW.

2.3 Synthesis and characterization of AgNPs

AgNPs were prepared according to previous work [32]. In short, 36 mg $AgNO_3$ was added to 200 mL of water and boiled under constant stirring. Then, trisodium citrate (4 mL, 1%) solution was added to the above solution quickly and boiling continued for another 30 min. Let the flask chill to room temperature, a green-gray colloid was acquired. Finally, the colloidal AgNPs were stored at 4°C for later use.

2.4 Preparation of Hg^{2+} standard solution and samples

$HgCl_2$ was dissolved in deionized water to make a 1 mM solution. A set of Hg^{2+} solutions with different concentrations were obtained by diluting 1 mM $HgCl_2$ solution. Drain water from a tap was collected in Shenyang City, Liaoning Province, China. The samples passed a 0.22 μm filter membrane to remove impenetrable matter for the later experiments.

2.5 Detection for Hg^{2+}

DTZ solution (20 μL), AgNPs (60 μL), and Hg^{2+} (20 μL) or spiked water solution of different concentrations were transferred to a centrifuge tube in turn, and SERS detection performed after fully sonicating and mixing at room temperature. The intensity of SERS change of DTZ at 1590 cm^{-1} was elected as a basis for quantification. Each experiment was performed three times in parallel.

3 Results And Discussion

3.1 SERS measurement of DTZ and DTZ-Hg^{2+}

Figure 2a shows the UV-vis absorption spectrum of AgNPs at 420 nm, and the TEM image showed that the size of uniform spherical AgNPs is about 30nm, which demonstrated the successful synthesis of AgNPs. The UV-vis peaks of AgNPs and DTZ shifted, indicating that DTZ was successfully adsorbed on the AgNPs surface. The SERS signal of DTZ, DTZ with Hg^{2+} and ethanol are in Figure 2b, in which the main SERS signals of DTZ were located at 510, 855, 994, 1156, 1219, 1310, 1377 and 1590 cm^{-1} [33]. Comparing these signal peaks, it is found that the SERS peak at 1590 cm^{-1} which is attributed to the C=N vibration of DTZ, has obvious changes, so it is the most suitable for use as a basis for quantitative analysis. Comparing the blue and the red lines, after adding Hg^{2+}, the SERS intensity of the DTZ molecules reduced significantly. This is substantially due to the change in number of DTZ molecules adsorbed on the SERS active sites. The SERS signal of DTZ was dramatically enhanced because the DTZ molecules drew closer to the SERS active sites through the Ag–N bond. However, after the addition of Hg^{2+}, the binding force between Hg^{2+} and DTZ is stronger than that with AgNPs, which leads to the desorption of DTZ molecules from SERS active sites. As a result, fewer DTZ molecules were left on the AgNPs surface and the SERS signal intensity was reduced.

3.2 Optimization of the analytical conditions

To increase the sensitivity of this method, we optimized the experimental parameters. The volume of AgNPs will affect the analytical performance. The number of AgNPs is very important for enhancing the SERS signal. Figure 3a shows the intensity of the SERS signal of DTZ at 1590 cm^{-1}, with the volumes of AgNPs solution from 30 to 70 μL. Upon the increase in the volume of AgNPs, the corresponding Raman signal increased. However, when the volume exceeded 60 μL, the SERS signal achieved a steady value, which proved that DTZ is completely adsorbed on the AgNPs. Therefore, 60 μL AgNPs were chosen for the detection of Hg^{2+}. In this method, DTZ will connect AgNPs and Hg^{2+}, so we explored the influence of DTZ concentration. As shown in Figure 3b, the SERS signal reached a maximum value when the concentration of DTZ is 10^{-4} M. Thus, we fixed 10^{-4} M as the optimum condition. Mixing time plays a critical part in this detection process, so we optimized the mix time. Figure 3c shows that after mixing for

8 min the signal tends to be stable, demonstrating that DTZ was entirely integrated with Hg^{2+}. So, we chose 8 min as the optimized mix time.

3.3 Selectivity for the DTZ-Hg^{2+} system

In order to study the selectivity of this method, various other environment–related metal ions were appraised (such as Fe^{3+}, Cu^{2+}, Al^{3+}, Na^{+}, K^{+}, Ni^{2+}, Bi^{3+} and Pb^{2+}). Figure 4a shows the comparison to SERS spectra of the Hg^{2+} and other ions, on the basis of the low binding affinity of DTZ to other ions, the SERS signal of DTZ did not reduce significantly in the presence of the other ions, which indicated the DTZ sensors for Hg^{2+} detection had an excellent selection. In the presence of the above substances, the corresponding SERS signal intensities of the 1590 cm^{-1} peak of DTZ are presented in the form of a histogram (Figure 4b). Hg^{2+} and mixed groups reveal distinctly low column heights.

3.4 Quantitative SERS detection of Hg^{2+}

To assess the sensitivity and potential quantitative analysis application of the proposed method, we measured different concentrations of Hg^{2+} standard samples. Under the optimum conditions, the present method showed a linear relationship for Hg^{2+} concentrations and the SERS peak in the range of 10^{-4} M to 10^{-8} M with a limit of detection of 9.83×10^{-9} M, which conforms to the equation $Y = 1096.3961X + 15738.17866$ ($R^2 = 0.999$). The relevance between the SERS signal intensity and Hg^{2+} concentration is shown in Figure 5. In the comparison, the experimental results of some other methods for measuring Hg^{2+} are listed in Table 1, which showed that our method is simpler and faster. More importantly, the detection result is inferior to the limit of 10 ppb (4.98×10^{-8} M) in drinking water recommended by the World Health Organization.

Table 1
A comparison between the previously reported method and the current method for detecting Hg^{2+}.

Method	Linear range (μmol / L)	LOD (μmol / L)	Reference
SERS	0.1-0.01	0.009	This work
SERS	–	0.5	[34]
Electrochemistry	0.1–2.0	0.1	[35]
Colorimetry	–	0.498	[36]
Colorimetry	–	0.05	[37]
Fluorescence	0.05–0.8	0.015	[38]
Fluorescence	–	0.011	[39]
ELISA	0.05-50.0	0.048	[40]

3.5 Reproducibility of the Hg^{2+} detection

To assess the reproducibility of the system, 20 different points were randomly gathered for testing under the optimum experimental conditions. The results are shown in Figure 6. It is worth noting that the SERS intensity at 1590 cm^{-1} is relatively uniform. From Figure 6b, we find that the relative standard deviation of the 20 sets of data is less than 5%, which proves that the SERS sensor proposed here article has satisfactory reproducibility.

3.6 Analysis of Hg^{2+} in tap-water samples

To demonstrate the practicality of the developed SERS method, we detected the Hg^{2+} contents in tap water under the optimum conditions by the standard addition method. Different concentrations of Hg^{2+} were tested 3 times and the results are shown in Figure 7. We further evaluated a comparison of the developed SERS method and the conventional ICP–MS method and the related statistics are shown in Table 2, which indicates that the Hg^{2+} concentrations detected by the SERS sensor are very consistent with those measured by the classic ICP–MS method. The recovery for Hg^{2+} was 89–90%. The results showed that this method is reliable and applicable for the detection of Hg^{2+} in tap water.

Table 2

Determination of Hg^{2+} in tap-water samples via the SERS method and ICP–MS.

Samples	Spiked amount (μM)	SERS amount	SERS Recovery%	RSD% (n=3)	Spiked amount (μM)	ICP–MS amount	ICP–MS Recovery%
Tap–water	–	Not detected	–	–	–	Not detected	–
	10	9.77	90.31	1.65	10	9.63	89.96
	1	1.12	88.90	1.31	1	0.46	89.44
	0.1	0.10	89.53	0.43	0.1	0.09	89.12

4 Conclusion

In short, we developed a time–saving, high–sensitivity SERS sensor for detecting Hg^{2+}. This sensor works with excellent sensitivity via the special recognition of Hg^{2+} by DTZ, which is attributed to the following: first, DTZ itself has a high SERS signal that can be used for Hg^{2+} quantitative detection. Moreover, DTZ specifically captures Hg^{2+} forming a steady structure that can enhance the specificity of this method. More importantly, under the best conditions, SERS–based Hg^{2+} detection exhibited a limit of detection of 9.83×10^{-9} M. This sensor can detect Hg^{2+} in a broad range of concentrations. With these advantages, we anticipate this method will have fine potential in the detection of Hg^{2+} in complex water environments.

Declarations

Acknowledgments

This work was supported by the National Natural Science Foundation of China (Grant No. 11974152 and 21671089), the LiaoNing Revitalization Talents Program (Grant No. XLYC1807162), the Shenyang Highlevel Innovative Talents Program (RC200565), the Scientific Research Projects of Liaoning Provincial Department of Education (L2020002), the Liaoning Provincial Natural Science Foundation Joint Fund Project (2020–YKLH–22), the Science program of Liaoning Provincial Department of Education (LJKZ0097), the Intercollegiate cooperation project of colleges and universities of Liaoning Provincial Department of Education.

Statements and Declarations

Funding

This work was supported by the National Natural Science Foundation of China (Grant No. 11974152 and 21671089), the LiaoNing Revitalization Talents Program (Grant No. XLYC1807162), the Shenyang

Highlevel Innovative Talents Program (RC200565), the Scientific Research Projects of Liaoning Provincial Department of Education (L2020002), the Liaoning Provincial Natural Science Foundation Joint Fund Project (2020–YKLH–22), the Science program of Liaoning Provincial Department of Education (LJKZ0097), the Intercollegiate cooperation project of colleges and universities of Liaoning Provincial Department of Education.

Competing Interests

The authors have no relevant financial or non-financial interests to disclose.

Ethics approval

Not applicable.

Consent to participate

Not applicable.

Consent for publication

Not applicable.

Availability of data and material

All data generated or analysed during this study are included in this published article.

Code availability

Not applicable.

Authors' Contributions

All authors contributed to the study conception and design. Material preparation, data collection and analysis were performed by Na Guo, Guangda Xu, Qijia Zhang, Peng Song and Lixin Xia. The first draft of the manuscript was written by Na Guo and all authors commented on previous versions of the manuscript. All authors read and approved the final manuscript.

References

[1] P. Amit, K. Ajay, H. Zhong (2018) Adverse effect of heavy metals (As, Pb, Hg, and Cr) on health and their bioremediation strategies: a review. Int. Microbiol. 21:97–106

[2] N. Abdu, A. Abdullahi, A. Abdulkadir (2017) Heavy metals and soil microbes. Environ. Chem. Lett. 15:65–84

[3] R. Kothalam, P. Perumal, R. Ayyanu (2019) Magnetic core-shell fibrous silica functionalized with pyrene derivative for highly sensitive and selective detection of Hg (II) ion. J. DISPER. SCI. TECHNOL. 40:1368-1377

[4] B.Q. Hao, X.F. Bu, J.W. Wu, Y.R. Ding, L.X Zhang, B. Zhao, Y. Tian (2020) Determination of Hg^{2+} in water based on acriflavine functionalized AgNPs by SERS. MICROCHEM. J. 155:104736

[5] J. Wang, B.L. Deng, H. Chen, X.R. Wang, J.Z. Zheng (2009) Removal of Aqueous Hg(II) by Polyaniline: Sorption Characteristics and Mechanisms. Environ. Sci. Technol. 43:5223–5228

[6] A. Rajeshwari, D. Karthiga, C. Natarajan, M. Amitava (2016) Anti-aggregation-based spectrometric detection of Hg(II) at physiological pH using gold nanorods. Mat. Sci. Eng. C-Mater 67:711–716

[7] G. GianPaolo, A.M. Caterina, P. La (2008) Molecular mechanisms triggered by mercury. Toxicology 244:1–12

[8] O. Juma, R. F. Christopher, C. Christopher (2021) Concentration-dependent health effects of air pollution in controlled human exposures. Environ. Int. 150:106424

[9] L.Y. Yu, L.Y. Zhang, G.J. Ren, S. Li, B.Y. Zhu, F. Chai, F.Y. Qu, C.G. Wang, Z.M. Su (2018) Multicolorful fluorescent-nanoprobe composed of Au nanocluster and carbon dots for colorimetric and fluorescent sensing Hg^{2+} and Cr^{6+}. Sensor. Actuat. B-Chem. 262:678–686

[10] X.K. Li, Y.L. Zhang, Y.L. Chang, B. Xue, X.G. Kong, W. Chen (2017) Catalysis-reduction strategy for sensing inorganic and organic mercury based on gold nanoparticles. Biosens. Bioelectron. 92:328–334

[11] Y.Y. Qi, F.R. Xiu, G.D. Yu, L.L. Huang, B.X. Li (2017) Simple and rapid chemiluminescence aptasensor for Hg^{2+} in contaminated samples: A new signal amplification mechanism. Biosens. Bioelectron. 87:439–446

[12] R.A. Konstantin, B.A. Mikhail, M.V. Alexander, T.A. Zaual, B.Y. Mikhail, S.A. Karina (2018) A novel photochemical vapor generator for ICP–MS determination of As, Bi, Hg, Sb, Se and Te. Talanta 187:370–378

[13] B.H. Daisa, S.O. Alexander, P.C. Camila, O.Q. Eliézer, R.S. Anderson, V.A. Mariana (2021) Determination of Hg in xanthan gum by CV AAS after acid decomposition using reflux system. Food Hydrocolloid. 118:106802

[14] X.L. Chai, X.J. Chang, Z. Hu, Q. He, Z.F. Tu, Z.H. Li (2010) Solid phase extraction of trace Hg(II) on silica gel modified with 2–(2–oxoethyl)hydrazine carbothioamide and determination by ICP–AES. Talanta 82:1791–1796

[15] B.J. Martin, H.J. Steve, W.J. Paul (1994) Determination of trace metals in sea-water and the on-line removal of matrix interferences by flow injection with inductively coupled plasma mass spectrometric

detection. J. Anal. At. Spectrom. 9:935–938

[16] Q.X. Zhou, M. Lei, Y.L. Liu, Y.L. Wu, Y.Y. Yuan (2017) Simultaneous determination of cadmium, lead and mercury ions at trace level by magnetic solid phase extraction with Fe@Ag@Dimercaptobenzene coupled to high performance liquid chromatography. Talanta 175:194–199

[17] L. Luo, Z.Y. Zhang, Y.H. Chen, L.X. Zhang, X.F. Bu, H.Q. Zhang, Y. Tian (2017) Simple and rapid surface-enhanced Raman Spectroscopy assay for safranine T and its application in highly sensitive determination of mercury (□). Int. J. Environ. An. Ch. 97:1178–1191

[18] J. Sehan, K.Y. Woo, H.H. Sung, S. Jiye, K. Yonghwan, L. Miran, P.S. Ki (2019) Fluorescence, turn–on detection of melamine based on its dual functions as fluorescence enhancer of DNA–AgNCs and Hg(II)–scavenger. Artif. Cell. Nanomed. B 47:621–625

[19] Y.L. Cui, Y.Q. Hao, Y.T. Zhang, B.X. Liu, X. Zhu, P. Qu, D.L. Li, M.T. Xu (2016) A water–soluble and retrievable ruthenium–based probe for colorimetric recognition of Hg(II) and Cys. Spectrochim. Acta. A. 165:150–154

[20] S. Li, L.G. Xu, W. Ma, H. Kuang, L.B. Wang, C.L. Xu (2015) Triple Raman Label–Encoded Gold Nanoparticle Trimers for Simultaneous Heavy Metal Ion Detection. Small 11:1613–6810

[21] Q. Hao, M.Z. Li, J.W. Wang, X.C. Fan, J. Jiang, X.X. Wang, M.S. Zhu, T. Qiu, L.B. Ma, P.K. Chu, S.G. Oliver (2020) Flexible Surface–Enhanced Raman Scattering Chip: A Universal Platform for Real-Time Interfacial Molecular Analysis with Femtomolar Sensitivity. ACS Appl. Mater. Inter. 12:54174–54180

[22] D. Gokhan, U. Hakan, Y. Mehmet, C. Merve , A.A. Husniye , B. Fatih (2018) Surface-enhanced Raman spectroscopy (SERS): an adventure from plasmonic metals to organic semiconductors as SERS platforms. J. Mater. Chem. C 6:5314–5335

[23] N.Y. Hao, M. Chen, H. Yang, R.L. Li, Q. Liu, Y.Q. Zhu, L.M. Wang, M. Peng, J. Xiang, X.Q. Chen (2020) “Pomegranate-Like” Plasmonic Nanoreactors with Accessible High–Density Hotspots for in Situ SERS Monitoring of Catalytic Reactions. Anal. Chem. 92:4115–4122

[24] Y. Wang, C. Zhou, W. Wang, D.D. Xu, F.Y. Zeng, C. Zhan, J.H. Gu, M.Y. Li, W.W. Zhao, J.H. Zhang, J.H. Guo, H.H. Feng, X. Ma (2018) Photocatalytically Powered Matchlike Nanomotor for Light–Guided Active SERS Sensing. Angew Chem. Int Edit. 40:13110–13113

[25] K. Surabhi, C. Thomas, Y. Kuang (2022) Silver enriched silver phosphate microcubes as an efficient recyclable SERS substrate for the detection of heavy metal ions. J. Colloid. Interf. Sci. 605:173–181

[26] Y. Gao, L.F. Li, X. Zhang, X.N. Wang, W. Ji, J.Z. Zhao, O. Yukihiro (2019) CTAB–triggered Ag aggregates for reproducible SERS analysis of urinary polycyclic aromatic hydrocarbon metabolites. Chem. Commun. 55:2146–2149

[27] Y. Tehseen, P .Hongbin, D.W. Sun (2019) Fabrication of silver-coated gold nanoparticles to simultaneously detect multi–class insecticide residues in peach with SERS technique. Talanta 196:537–545

[28] C. Jeongan, L. Jiwon, J.H. Jae (2020) Fully integrated optofluidic SERS platform for real–time and continuous characterization of airborne microorganisms. Biosens. Bioelectron. 169:112611

[29] L. Qi, M.S. Xiao, F. Wang, L.H. Wang, W. Ji, T.T. Man, A. Ali, K. Naziruddin, P. Govindasami, R. Mostafizur, A. Abdulaziz, X.M. Qu, H. Pei, C. Wang, L. Li (2017) Poly–cytosine–mediated nanotags for SERS detection of Hg^{2+}. Nanoscale 9:14184–14191

[30] J.B. Cui, M.Y. An, L.Y. Wang (2013) Nanocomposite–based rapid, visual, and selective luminescence turn-on assay for Hg^{2+} sensing in aqueous media. Talanta 115:512–517

[31] M.A. Kiwan, M.F. Hassan, W. Hamdan (1989) Studies on Tetramethyldithizone Isomers and Their Reactions with Metal Ions. B. Chem. Soc. Jpn. 62:325–329.

[32] X. Gu, C.P. Jon (2015) Surface-Enhanced Raman Spectroscopy-Based Approach for Ultrasensitive and Selective Detection of Hydrazine. Anal. Chem. 87:6460–6464

[33] S. Sujittra, W. Nootcharin, K. Mayuso, S. Siriprapa, T. Narissara (2021) Raman enhanced scattering and DFT studies on the adsorption behaviour of dithizone on silver nanoparticle. Inorg. Chem. Commun. 126:108480

[34] H. Donghoon, L.Y. Sung, K.J. Beom, L.L. Piao, C.D. Taek (2010) Mercury(ii) detection by SERS based on a single gold microshell. Chem. Commun. 46:5587–5589

[35] H. Donghoon, K.R. Yang, O.W. Jeong, K.H. Tae, M.K. Rakesh, K.S. Jong, K. Hasuck (2009) A regenerative electrochemical sensor based on oligonucleotide for the selective determination of mercury(□). Analyst 134:1857–1862

[36] C. Ridhima, D. Abhishek, D.K. Anil, K. Sudhir, M. Nandita (2021) 2-thiazoline-2-thiol functionalized gold nanoparticles for detection of heavy metals, Hg(II) and Pb(II) and probing their competitive surface reactivity: A colorimetric, surface enhanced Raman scattering (SERS) and x-ray photoelectron spectroscopic (XPS) study. Colloid. Surface. A. 615:126279

[37] T. Li, S.J. Dong, E.K. Wang (2009) Label–Free Colorimetric Detection of Aqueous Mercury Ion (Hg^{2+}) Using Hg^{2+}–Modulated G–Quadruplex–Based DNAzymes. Anal. Chem. 81:2144–2149

[38] W.Y. Xie, W.T. Huang, H.Q. Luo, N.B. Li (2012) CTAB–capped Mn–doped ZnS quantum dots and label–free aptamer for room-temperature phosphorescence detection of mercury ions. Analyst 137:4651–4653

[39] L. Luo, T. Song, H.Q. Wang, Q.H. Yuan, S.H. Zhou (2018) A highly selective fluorescence sensing platform for nanomolar Hg(II) detection based on cytosine derived quantum dot. Spectrochim. Acta. A. 193:95-101

[40] X.J. Zhan, T. Xi, P. Zhou (2013) Indirect Competitive Immunoassay for Mercury Ion Determination Using Polyclonal Antibody Against the Hg–GSH Complex. Environ. Forensics 14:103–108

Figures

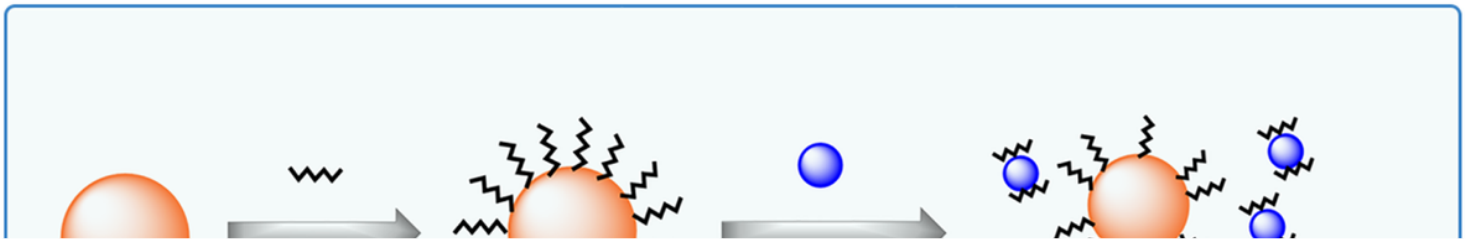

Figure 1

Schematic illustration of Hg^{2+}sensor.

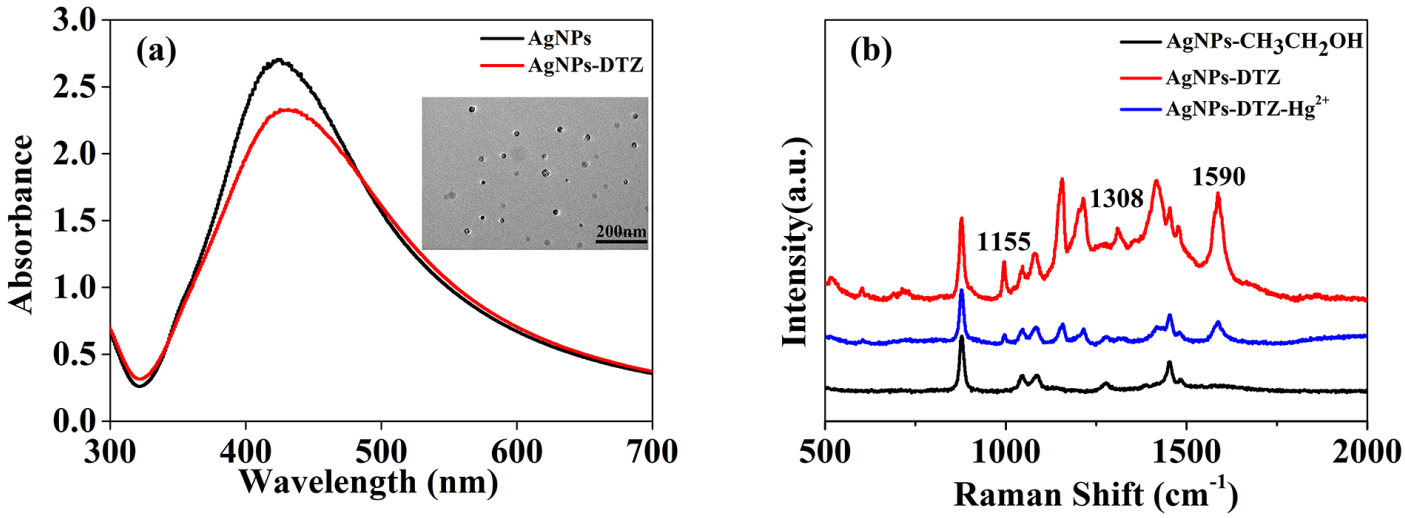

Figure 2

(a) UV-Vis spectrum of the AgNPs, AgNPs and DTZ. Inset shows the TEM images of the AgNPs. (b) SERS spectra of AgNPs and ethanol, DTZ and DTZ in the presence of 10^{-4} M Hg^{2+}.

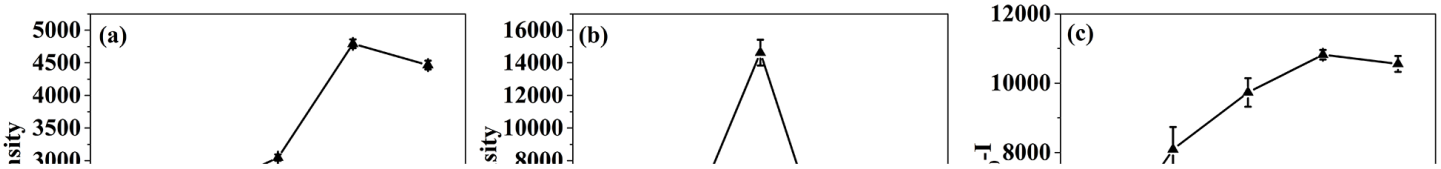

Figure 3

(a) Optimization of the volume of AgNPs. (b) The concentration of DTZ. (c) The mixed time. The error bars stand for the standard deviations based on at least three independent measurements.

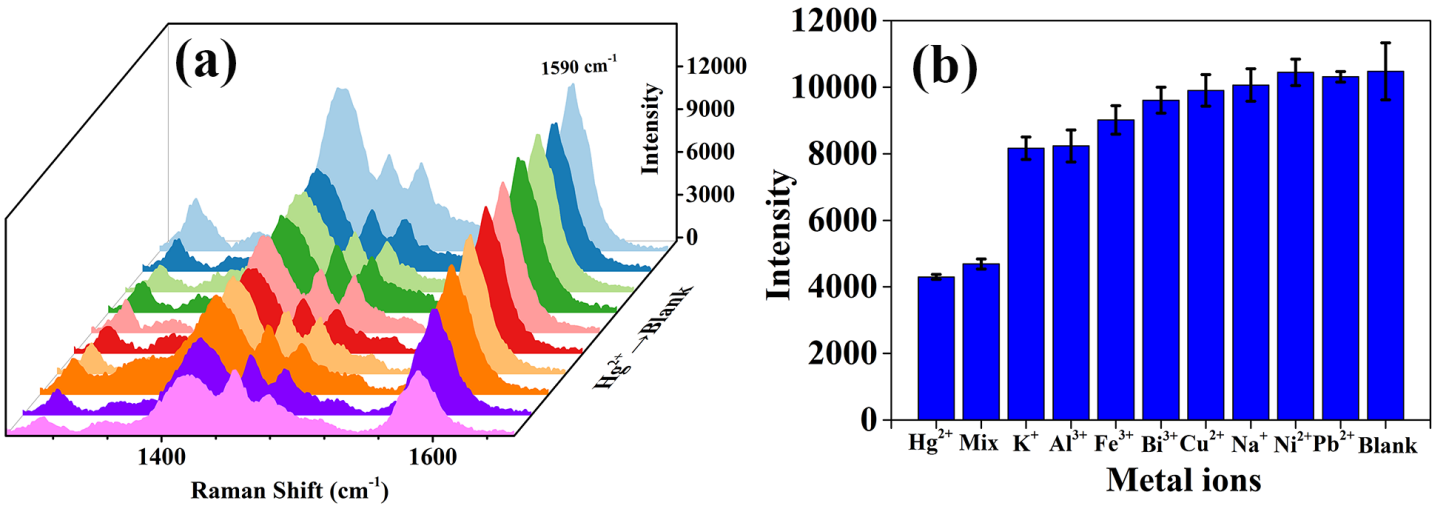

Figure 4

The sensor selectivity and anti-interference ability for detecting Hg^{2+}.

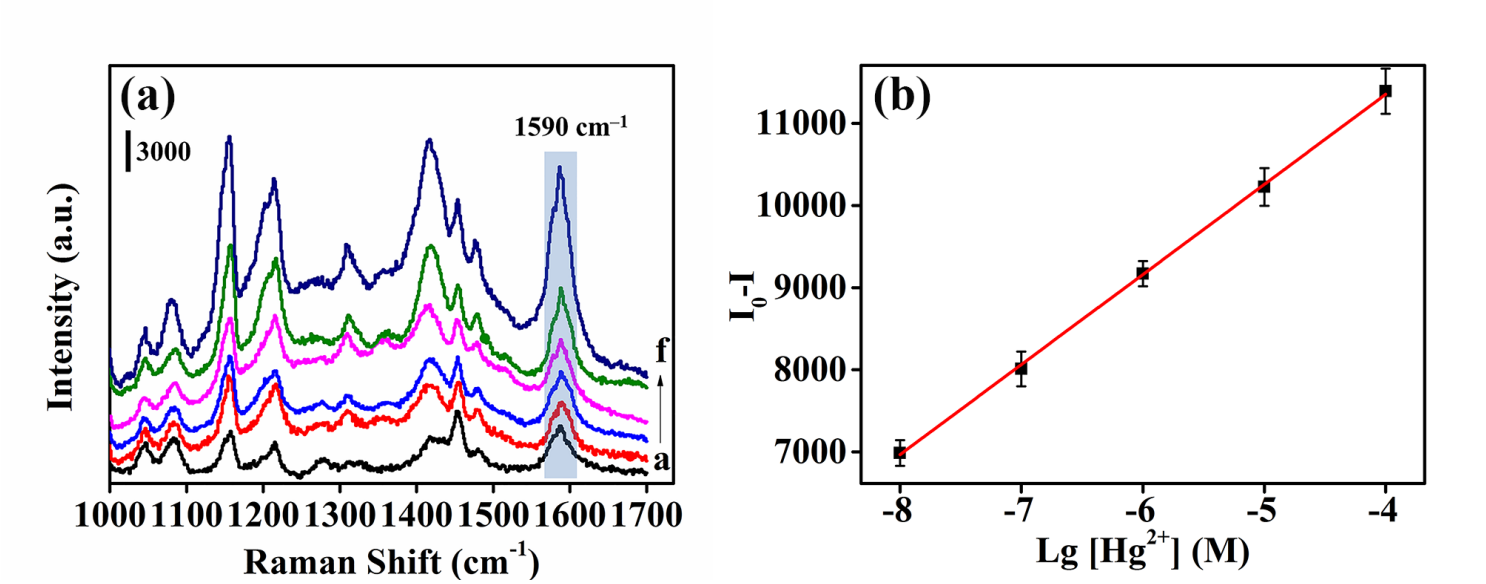

Figure 5

(a) The SERS spectra of DTZ mixed with different concentration of Hg^{2+} (from a to f are 10^{-4}, 10^{-5}, 10^{-6}, 10^{-7}, 10^{-8} and 0 M). (b) The plot of corresponding intensity.

Figure 6

(a) The SERS intensity at 1590 cm^{-1} was measured from 20 random positions. (b) A series of SERS spectra of 10^{-5} M Hg^{2+} solution from 20 random positions.

Figure 7

Detect the SERS spectra of different concentrations of Hg^{2+} in tap water.